Journal of Neural Engineering

PURPOSE-LED PUBLISHING™

PAPER • OPEN ACCESS

CLAS-hdEEG: high-density EEG software platform for real-time delta wave detection and closed-loop auditory stimulation

To cite this article: Hanieh Bazregarzadeh *et al* 2026 *J. Neural Eng.* **23** 026010

View the article online for updates and enhancements.

You may also like

- Oligodendrocyte-specific *fus* depletion preserves CA1 single-unit fidelity and stabilizes network dynamics during chronic recording
Steven M Wellman, Kelly Guzman, Naofumi Suematsu et al.
- Microglia surveillance is directed toward neuron activation during sustained intracortical microstimulation
Colin Preszler, Kevin C Stieger, Keying Chen et al.
- Computational modeling for precision targeting of conductivity-clamped gene electrotransfer within the striatum of the human brain
Keng-Yin Lai, Stephen L Mow, Mathumathi Manoharan et al.

This content was downloaded from IP address 142.137.141.84 on 22/04/2026 at 21:02

Journal of Neural Engineering

Check for updates

OPEN ACCESS

RECEIVED
17 November 2025

REVISED
3 March 2026

ACCEPTED FOR PUBLICATION
6 March 2026

PUBLISHED
17 March 2026

Original content from this work may be used under the terms of the Creative Commons Attribution 4.0 licence.

Any further distribution of this work must maintain attribution to the author(s) and the title of the work, journal citation and DOI.

PAPER

CLAS-hdEEG: high-density EEG software platform for real-time delta wave detection and closed-loop auditory stimulation

Hanieh Bazregarzadeh[1,6], **Clara Pic Roca**[1,2,6], **Antonio Martin**[1], **Karine Lacourse**[1], **Jean-Marc Lina**[1,3], **Julie Carrier**[1,4] and **Catherine Duclos**[1,2,5,*]

[1] Center for Advanced Research in Sleep Medicine (CARSM), Hôpital du Sacré-Coeur de Montréal, Centre intégré universitaire de santé et de services sociaux du Nord de l'Île-de-Montréal, Montréal, Canada
[2] Department of Neuroscience, Faculty of Medicine, Université de Montréal, Montréal, Canada
[3] Department of Electrical Engineering, École de Technologie Supérieure, Montréal, Canada
[4] Department of Psychology, Université de Montréal, Montréal, Canada
[5] Department of Anesthesiology and Pain Medicine, Faculty of Medicine, Université de Montréal, Montréal, Canada
[6] These authors contributed equally to this work.
[*] Author to whom any correspondence should be addressed.

E-mail: catherine.duclos@umontreal.ca

Keywords: auditory stimulation, real-time delta wave detection, closed-loop system, EGI Net Amp 300, high-density EEG

Abstract

Objective. Closed-loop auditory stimulation (CLAS) can enhance slow oscillations during non-rapid eye movement sleep; however, its broader use has been limited by technical and temporal constraints. We introduce and validate **CLAS-hdEEG**, a high-density electroencephalographic (hd-EEG) software platform integrated within the Magstim EGI environment, capable of real-time delta wave detection and phase-targeted auditory stimulation with low detection-to-stimulation latency, achieved through event-based detection of delta wave extrema. *Approach.* The CLAS-hdEEG software continuously streams 128-channel EEG data, applies an online moving average filter to Fz for real-time delta wave detection, and triggers brief pink noise bursts at the detected peak or trough of ongoing oscillations. Detection thresholds were based on established amplitude crossings, a minimum peak-to-peak difference of 75 μV, and duration limits of 160–1700 ms. Synchronization between neural detection and stimulus onset was verified using digital input hardware (DIN) markers recorded by the EGI acquisition system. The system was validated in 14 healthy participants during N3 sleep under peak, trough, and sham stimulation conditions. Phase-targeting success was defined as auditory bursts occurring within predefined 90° phase windows of the oscillation (0°–90° for in-phase blocks and 180°–270° for anti-phase blocks). *Main results.* Across all sessions, auditory stimuli were delivered with a mean detection-to-stimulation latency of 20.03 ± 0.5 ms and an overall phase-targeting success rate of 0.913, indicating that 91.3% of stimuli occurred within the predefined 90° target phase windows. Online and offline detections showed strong agreement ($F1 \approx 0.80$), confirming that real-time processing preserved the fidelity of offline algorithms. *Significance.* This study establishes the technical and temporal validity of CLAS-hdEEG, the first hd-EEG software platform for CLAS within the EGI environment. By combining low detection-to-stimulation latency with high-density spatial sampling, this framework provides a robust and extensible platform for investigating how auditory stimulation interacts with large-scale neural dynamics across diverse states of consciousness.

© 2026 The Author(s). Published by IOP Publishing Ltd

1. Introduction

1.1. Neurophysiological constraints for closed-loop stimulation of delta dynamics

1.1.1. Delta events as a target for real-time detection

Closed-loop stimulation of brain activity during sleep must operate within well-defined neurophysiological constraints. During non-rapid eye movement (NREM) sleep, cortical activity is dominated by high-amplitude, low-frequency slow wave activity in the delta range (∼0.5–4 Hz) [1–3], reflecting alternating periods of neuronal depolarization and hyperpolarization across large cortical populations [1, 4, 5]. From a mechanistic standpoint, delta activity encompasses both slow waves (1–4 Hz; SWs) and slow oscillations (<1 Hz; SOs). Because of their strong association with sleep depth and neuronal bistability, delta waves are widely quantified through spectral and event-based metrics such as delta wave power, peak-to-peak amplitude, slope, and event rate [6, 7]. Together, these metrics provide measurable features for real-time detection and modulation.

1.1.2. Functional relevance of delta dynamics for system validation

Delta waves provide a well-defined and technically advantageous signal class for validating real-time closed-loop electroencephalographic (EEG) systems. Their large amplitude, stereotyped waveform morphology, and low-frequency temporal structure make delta activity particularly suitable for benchmarking detection accuracy, timing precision, and phase specificity in online signal-processing pipelines. These properties enable systematic comparison between real-time detections and offline reference analyses, allowing objective assessment of algorithmic fidelity and end-to-end system performance [8, 9]. From a systems perspective, delta waves exhibit constrained amplitude ranges, duration bounds, and phase relationships that can explicitly be incorporated into detection criteria. As a result, deviations in event timing, threshold crossings, or phase alignment can be quantified relative to known signal characteristics, providing clear performance bounds for real-time modulation architectures. This makes delta dynamics a useful reference for evaluating the stability and robustness of closed-loop operations across extended recordings [9, 10].

Beyond its utility as a validation signal for closed-loop system development, delta-band activity has been associated with large-scale physiological processes related to sleep and cortical regulation. Delta dynamics contribute to restorative and mnemonic functions of sleep [11, 12], and their amplitude and frequency have been linked to global synaptic downscaling mechanisms that renormalize cortical excitability following wakefulness [13]. In addition, delta events support communication during memory consolidation [14–16]. More generally, delta-band activity correlates with homeostatic processes and recovery [17], including metabolic clearance [18], immune system regulation [19], and post-sleep vigilance [20]. Decreased delta dynamics have been reported in aging, insomnia, and clinical populations [21–23], motivating continued interest in approaches capable of detecting and modulating these events with higher temporal precision. These observations provide a broad rationale for developing robust and generalizable closed-loop EEG platforms.

1.2. Design requirements for modulation of delta waves

1.2.1. Existing neuromodulation approaches and technical constraints

Several non-invasive neuromodulation modalities have been tested to modulate delta wave dynamics. For example, Marshall *et al* (2006) [24] showed that frontally applied slow-oscillatory transcranial direct current stimulation (so-TDCS; 0.75 Hz) during NREM increased delta wave dynamics and improved memory recall. Transcranial magnetic stimulation (TMS), including repetitive protocols targeting prefrontal regions, has also been shown to transiently induce or enhance slow oscillatory and delta activity, with associated improvements in sleep continuity and sleep depth, particularly in insomnia populations [25, 26]. Among sensory approaches, closed-loop auditory stimulation (CLAS) delivers brief auditory sounds phase-targeted to the ongoing delta wave. The work by Ngo *et al* [27] demonstrated that such stimulation synchronized with the peak of the wave (*in-phase* stimulation) amplifies delta waves and improves declarative memory. Subsequent studies refined the timing of the algorithms and extended the method to older adults, clinical and neurological populations, naps, and at-home settings [28–33]. More recent work has expanded CLAS beyond behavioral outcomes, providing the neurophysiological evidence that *in-phase* auditory stimulation reinforces cortical up-states, enhances large-scale synchronization, and modulates slow-wave propagation across distributed cortical networks [34]. Comprehensive methodological guidelines have since been proposed, outlining the optimal detection, timing, and safety parameters for CLAS [10, 35]. In parallel, both empirical and review work have emphasized timing precision, system latency, and validation of phase alignment as critical determinants of CLAS efficacy and cross-study comparability [8, 9]. Despite these advances, reproducibility and cross-platform comparison remain limited by heterogeneity in system architectures, stimulation control strategies, and the type of timing validation performed.

Notably, a recent meta-analytic review reported that the magnitude of reported memory benefits from acoustic closed-loop stimulation varies across publication years and has been discussed in the context of a potential decline effect [36]. Importantly, early landmark studies demonstrated robust enhancements of slow oscillatory activity and memory performance when stimulation was precisely timed to the targeted phase [27, 37]. Together, these observations highlight the need for rigorous and transparent reporting of timing precision, end-to-end latency, and phase-alignment validation to support cross-study comparability and reproducibility across CLAS platforms.

While hd-EEG has been combined with both open-loop rhythmic auditory stimulation (e.g. Auditory Steady State Responses; ASSR) [38] and CLAS protocols, these implementations typically relied on external or wearable devices for real-time detection, with high-density EEG (hd-EEG) used primarily for offline analysis or validation [39–42].

1.3. System-level limitations of current CLAS implementations

1.3.1. Restricted spatial sampling

Most CLAS studies rely on a single frontal EEG electrode for online event detection [27, 32], which precludes the analysis of the spatial dynamics of delta waves. However, delta waves are known to exhibit marked regional variability in amplitude, slope, and timing across the cortex, often propagating as traveling waves from frontal to posterior regions [2, 43]. This spatial heterogeneity implies that a single electrode may not accurately capture the global phase or origin of a wave, potentially leading to suboptimal stimulation timing. Furthermore, local delta waves are common during NREM sleep [44, 45], underscoring the need for high-density recordings to distinguish global versus local events.

hd-EEG enables precise mapping of these spatial dynamics, revealing that delta activity can arise independently across cortical regions and that wave propagation delays vary by tens of milliseconds across sites [7, 46]. Such a distributed characterization is essential to determine whether stimulation at a single site modulates only local versus global oscillatory events. Broader spatial sampling is therefore critical for understanding and effectively modulating the distribution dynamics of delta activity.

Beyond spatial sampling, hd-EEG offers additional advantages over classical 10/20 EEG systems for advanced analyses, including functional connectivity, graph-theoretical measures, microstate dynamics, and complexity and criticality analyses. Moreover, high-density recordings allow for more precise source localization and propagation analyses than lower-density systems. These analyses are particularly relevant for studying alterations in large-scale network organization that accompany altered states of consciousness, such as sleep, anesthesia, and disorders of consciousness [47–49].

1.3.2. Latency and synchronization limitations

The efficacy of CLAS critically depends on the latency between neural event detection and stimulus delivery. From an engineering perspective, this imposes a strict real-time constraint in which end-to-end latency directly determines intervention efficacy. Several studies have demonstrated high algorithmic efficiency and precise phase targeting using threshold-based or adaptive phase-tracking approaches, particularly in wearable or mobile systems [27, 50]. These works provide important insights into algorithmic performance and phase estimation accuracy. However, these metrics primarily quantify computational or algorithm-level delays and, in many cases, do not fully capture the complete end-to-end latency between neural detection and physical sound emission within laboratory-based hd-EEG systems, where additional delays arise from acquisition hardware, operating system scheduling, and audio output pathways [32, 38, 50–53].

1.3.3. Reproducibility and platform-dependency constraints

Another limitation in current CLAS systems, including the present implementation, is the dependence on hardware-specific EEG-based stimulation platforms, which can complicate cross-platform reproducibility and direct comparison between implementations. This limitation arises from reliance on manufacturer-specific hardware and software interfaces, which restrict direct access to low-level acquisition, timing, and stimulation components. Hardware-related factors such as amplifier latency, sampling architecture, operating system scheduling, and audio output pathways can introduce non-negligible delays that are rarely quantified or reported in a unified manner across systems.

While methodological advances in delta wave detection and phase-targeting algorithms have improved transparency at the signal-processing level [46], system-level validation of timing and synchronization remains heterogeneous across platforms. Recent open-source and wearable frameworks, such as the Portiloop system [54] and other low-channel adaptive approaches [51, 53] have made important progress toward algorithmic transparency, benchmarking, and hardware accessibility. However, many hd-EEG implementations have relied on external or parallel stimulation devices for real-time control, using hd-EEG primarily for offline recording and post-hoc validation rather than for integrated closed-loop operation.

As a result, fully integrated hd-EEG systems that combine real-time neural event detection, stimulation control, and explicit end-to-end latency validation at the system level within a single synchronized experimental platform remain scarce.

In parallel with these limitations, laboratory-grade hd-EEG systems such as the Magstim EGI environment are well established in sleep research employing high-density recordings and provide standardized acquisition pipelines with well-characterized signal properties across studies [7, 38–41]. While this does not mitigate the limitations associated with proprietary hardware architectures or restricted hardware access, it supports that the present framework is applicable within a commonly adopted experimental ecosystem for hd-EEG-based sleep research.

2. Rationale and objectives

2.1. System-design rationale

The limitations of existing CLAS systems have motivated the development of a new software framework capable of integrating hd-EEG acquisition with low-latency, phase-targeted auditory stimulation. The goal was to design a platform that could operate in real-time within the Magstim EGI environment while minimizing the temporal gap between neural detection and stimulus delivery, emphasizing accurate phase targeting in the delta frequency range ($\sim 0.5-4$ Hz).

Unlike many previous implementations restricted to low-channel EEG or offline analyses, the present system records 128 electrodes (expandable up to 256), enabling the rich spatial characterization of delta waves for subsequent analyses of propagation dynamics, regional specificity, and network coherence. In parallel, the real-time pipeline focuses on a single frontal electrode (Fz) for online delta wave detection, optimizing computational efficiency, and minimizing the system latency. This hybrid design preserves the temporal precision while capturing comprehensive neural data for post-hoc validation and future multi-channel extensions.

A central aspect of this work is the reduction in the delay between the detection of an ongoing delta wave and the emission of an auditory stimulus. Achieving millisecond-scale detection-to-stimulation latency required tight synchronization between acquisition, processing, and stimulation modules within the EGI infrastructure (Magstim EGI, NetStation Acquisition software, version 5.4.3, Eugene, OR, USA). This performance enables accurate phase-specific interventions, particularly stimulation near the peak (up-state) or trough (down-state) of the oscillatory cycle, without phase drift or timing uncertainty.

2.2. Engineering objectives and performance criteria

Our overarching objective was therefore to develop and validate a CLAS software that meets rigorous performance benchmarks for recall and precision, and is directly integrated into a hd-EEG system.

From an engineering perspective, a key objective was to achieve a detection-to-stimulation latency sufficiently short to preserve phase-specific auditory stimulation within the delta frequency range ($\sim$0.54 Hz). Based on the temporal properties of delta oscillations, the target design criterion was an end-to-end latency below 50 ms, corresponding to less than approximately 20% of a delta cycle at 4 Hz, ensuring that stimulation remains confined to the intended phase window despite variability in detection and triggering latency.

Specifically, the system was designed to fulfill the following criteria:

(1) **Delta wave detection-stimulation sensitivity**: Each stimulation block (*in-phase* and *anti-phase*) was required to achieve a detection sensitivity greater than 75%, as defined by the ratio between the number of successfully stimulated delta waves and the total number of delta waves detected offline.

(2) **Phase-targeting performance during stimulation blocks (figure 1)**:
   (a) *In-phase*: Auditory triggers during *in-phase* blocks were expected to occur between 0° and 90° of the oscillatory cycle for at least 60% of stimulated delta waves, and within the broader up-slope interval ($270° - 90°$) for at least 80% of stimulated delta waves.
   (b) *Anti-phase*: Auditory triggers during *anti-phase* blocks were expected to occur between 180° and 270° of the oscillatory cycle for at least 60% of stimulated delta waves, and within the broader down-slope interval ($90° - 270°$) for at least 80% of stimulated delta waves.

(3) **Sham condition**: The *Sham* stimulation block was designed not to deliver any auditory triggers.

3. Methods

3.1. Algorithm

The CLAS algorithm was implemented in Python version 3.9.6 using an asynchronous PyQt5 framework to ensure real-time EEG acquisition, signal processing, and auditory feedback. The algorithm continuously receives EEG data from the EGI Net Amp 300 amplifier (Magstim EGI, NetStation Acquisition software, version 5.4.3, Eugene, OR, USA), extracts and filters the Fz channel, detects

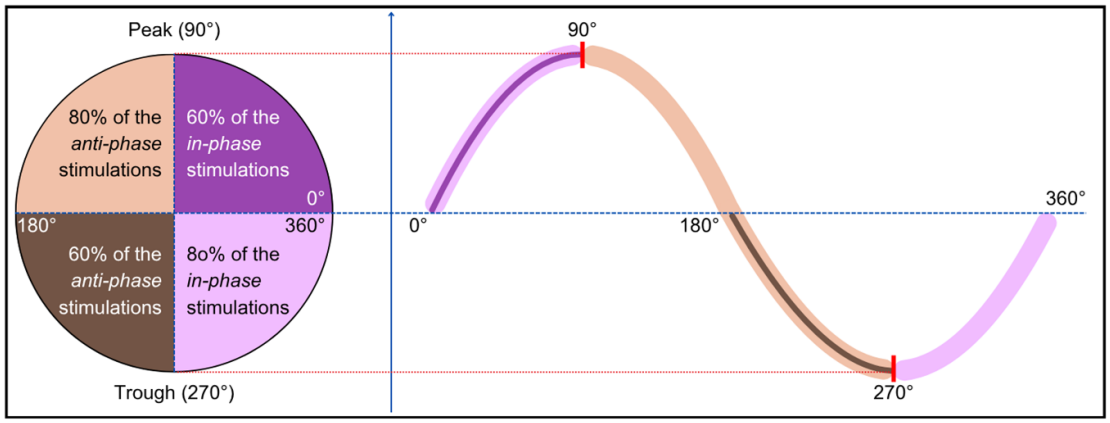

Figure 1. Phase-targeted auditory stimulation and predefined phase windows. The diagram illustrates the phase angles used for CLAS relative to the delta wave cycle. *In-phase* stimulation (purple) was expected to occur between 0° — 90° for at least 60% of stimuli, and within the broader 270° — 90° up-slope for at least 80% of stimuli. *Anti-phase* stimulation (brown) was expected to occur between 180° — 270° for at least 60% of stimuli, and within the broader 90° — 270° down-slope for at least 80% of stimuli.

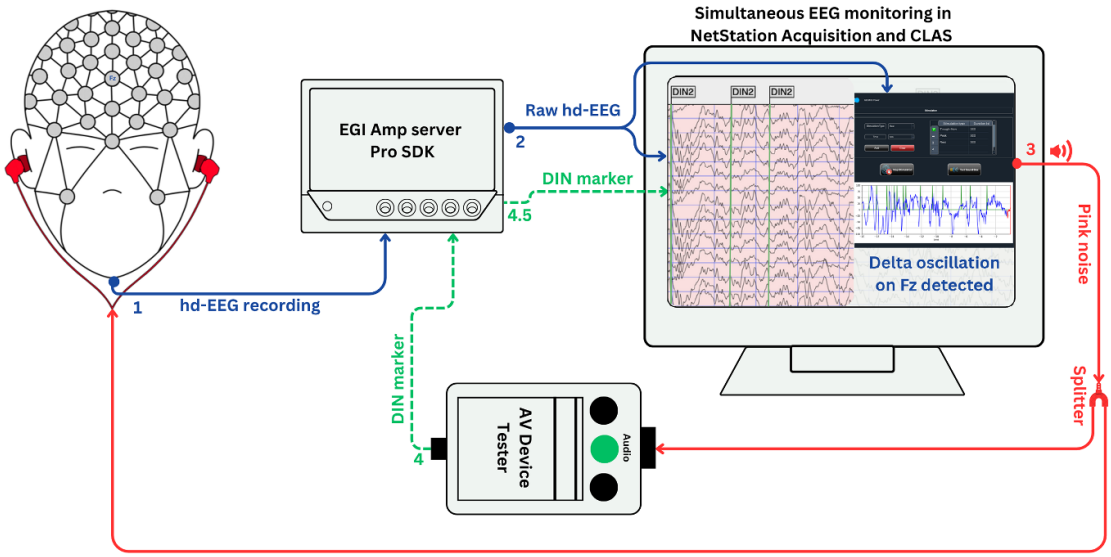

Figure 2. The CLAS system and experimental setup. Hd-EEG was recorded using a Magstim EGI Net Amp 300 with simultaneous data streaming to both the NetStation Acquisition software and the custom-designed CLAS application. The CLAS app performed real-time detection of delta wave extrema on the Fz channel and triggered auditory pink noise stimulation via earbuds. Each stimulation event was marked both internally and by an external Digital Input (DIN marker) trigger recorded in the EEG trace, enabling precise timing analysis of closed-loop responses.

delta wave extrema (peaks and troughs) based on predefined amplitude and duration criteria, and triggers auditory stimulation with millisecond-scale detection-to-stimulation latency. An overview of the complete CLAS-hdEEG system is shown in figure 2. EEG signals from the Magstim EGI Net Amp 300 were streamed simultaneously to the NetStation Acquisition software for recording and to a custom CLAS application for real-time processing. The CLAS app continuously analyzed the Fz channel to detect delta wave extrema and delivered auditory stimulation through calibrated earphones. Each event was marked by both internal and external hardware triggers to ensure precise synchronization between the EEG trace and sound onset. The use of a single electrode (Fz) as the real-time control channel reflects engineering constraints inherent to closed-loop operation. In CLAS systems, stimulation timing is commonly derived from a single, stable reference channel using event-based or phase-referenced criteria in order to minimize computational load and ensure low-latency triggering. Hd-EEG acquisition was nevertheless retained to allow full-bandwidth, multi-channel signal recording for offline processing and future use of the software framework.

Figure 3. Graphical user interface of the CLAS application. The CLAS app displays the continuously updated filtered Fz signal, detected delta wave events, and stimulation progress indicators. Operators can configure stimulation type (Peak, Trough, Rest), block duration, and audio testing directly through the interface.

3.2. Data acquisition and preprocessing

EEG packets were streamed via the AmpServer interface using asynchronous I/O to prevent blocking between acquisition and processing threads. Each incoming packet contained short data segments (1000 samples) from all channels from which the Fz signal was extracted and down-sampled to 500 Hz for real-time detection. The system ignored the first 100 packets from the moment of app activation to allow the baseline and filters to stabilize before the detection began. Two moving-average buffers were implemented to suppress slow drifts and high-frequency noise, while preserving the delta wave morphology:

Baseline (DC) buffer: a slow sliding window (2 s; 1000 samples) estimating the mean Fz amplitude used for DC removal. This step compensates for the electrode-dependent baseline offsets present in hd-EEG systems using a common reference (Cz), in which each channel exhibits a distinct DC potential due to reference configuration and impedance differences.

Smoothing buffer: a short-term moving average window (25 samples) applied to the DC-corrected signal to attenuate high-frequency fluctuations.

The resulting trace (filtered signal) was continuously updated and displayed on a graphical interface for online monitoring. Figure 3 illustrates the CLAS app interface during an active session, in which three stimulation blocks have been configured by the operator. Within the interface, users can test auditory playback, define the stimulation type (e.g. active or sham) and duration, and organize multiple stimulation blocks in a customizable order. Once the stimulation is started, the app automatically progresses through the predefined blocks sequentially, and each completed block is marked with a green check icon, whereas the active block in progress is indicated by an arrow. This setup allows for a flexible experimental design and clear visual tracking of the stimulation status throughout the session.

3.3. Parameter optimization for online filtering

The parameter values for the DC-removal and smoothing filters were determined through a combination of theoretical considerations and empirical validation to balance the signal fidelity, latency, and noise suppression. The DC-removal filter estimated the running mean of the Fz signal over a 2 s window (1000 samples at 500 Hz) and subtracted it from the raw signal. This operation behaves as a high-pass filter with a cutoff frequency given by

$$f_c = \frac{1}{2T} \tag{1}$$

where T is the length of the moving average window in seconds. For $T = 2$ s, the cutoff is approximately $f_c \approx 0.25$ Hz. This value was chosen because

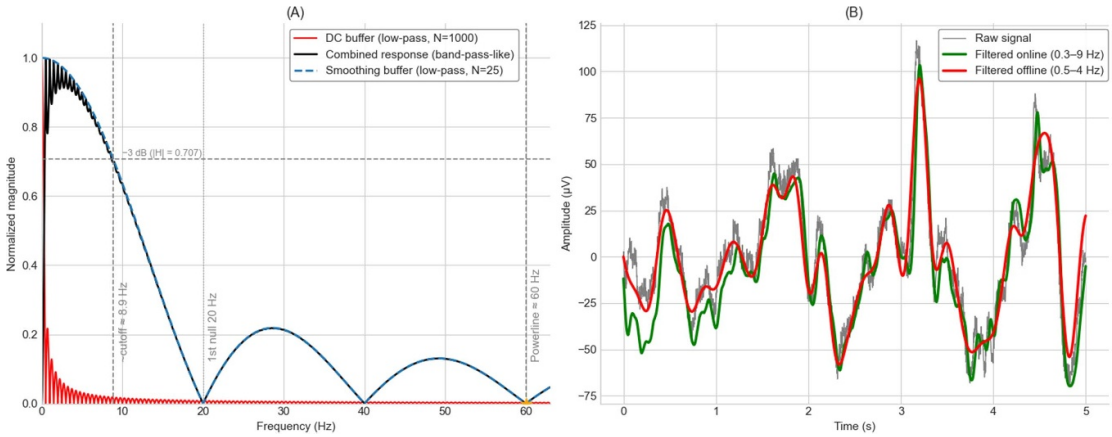

Figure 4. Frequency and time-domain validation of online filtering. (A) Frequency responses of the DC buffer (low-pass, 2 s = 1000 samples), the smoothing buffer (low-pass, 25 samples), and their combined band-pass-like response. Subtracting the slow DC estimate from the signal produces a high-pass component, which, when cascaded with the smoothing filter, yields a pass-band centered in the delta range (∼0.5–4 Hz). (B) Comparison of 5 s of raw, offline-filtered, and online-filtered Fz signals showing stable baseline correction, minimal delay, and effective attenuation of high-frequency and DC components. The online-filtered signal closely follows both the raw and offline-filtered signals, confirming accurate real-time performance of the implemented filters.

it efficiently removes very slow drifts and electrode-dependent DC offsets that are common in hd-EEG systems using a common reference (Cz), while preserving low-frequency components associated with delta wave activity.

A smoothing filter was implemented as a 25-sample moving average (50 ms at 500 Hz). The theoretical frequency response of a moving-average filter follows a sinc-shaped function, with its first spectral null at

$$f_0 = \frac{f_s}{N} \tag{2}$$

and its $-3\,dB$ cutoff frequency approximated by

$$f_c \approx 0.443\frac{f_s}{N} \tag{3}$$

where f_s is the sampling frequency and N is the window length (samples). For $f_s = 500$ Hz and $N = 25$, the first null occurs at $f_0 = 20$ Hz and the effective cutoff is $f_c \approx 0.443 \times (500/25)$ =8.86 Hz. This configuration, therefore, acts as a low-pass filter that preserves delta waves (<9 Hz) while attenuating higher-frequency activity such as alpha rhythm and muscle noise. A smaller window size would have allowed residual high-frequency and 60 Hz power-line components to remain, while a larger window would have introduced greater delay in the online signal due to increased filter latency.

Thus, the selected combination, a 2 s DC-removal filter (high-pass ∼ 0.25 Hz) and a 25-sample smoothing filter (low-pass ∼ 8.86 Hz), resulted in an effective band-pass response between approximately 0.25 Hz and 9 Hz, centered in the delta range ∼0.5–4 Hz most relevant for delta wave detection.

Figure 4(A) illustrates the frequency responses of the DC buffer (low-pass, 2 s = 1000 samples), the smoothing buffer (low-pass, 25 samples), and their combined response. Subtracting the slow DC estimate from the signal effectively produces a high-pass component that, when cascaded with the smoothing filter, yields a band-pass-like response centered in the delta range (∼0.5–4 Hz). This configuration attenuates both ultra-slow drifts (<0.3 Hz) and high-frequency components (>9 Hz), including 60 Hz power-line noise, while preserving the morphology of delta waves relevant to delta wave detection. The final parameters of DC window = 2 s and smoothing window of 25 samples yielded stable baseline correction, minimal latency relative to the raw signal, and effective suppression of high-frequency artifacts and DC offsets. Figure 4(B) demonstrates that the online-filtered signal closely follows both the unfiltered and offline-filtered signals, confirming accurate real-time tracking and proper online filtering.

3.4. Online delta wave detection

The CLAS-hdEEG system operates as a real-time closed-loop architecture in which ongoing EEG activity is continuously analyzed and directly used to trigger auditory stimulation without user intervention. Real-time detection of delta wave extrema was implemented using a state-machine architecture operating on the continuously updated, filtered Fz signal. At each iteration, the algorithm processed the most recent sample received from the amplifier and evaluated it against predefined amplitude and timing thresholds. Two independent detection conditions are available: *Peak* and *Trough*. All thresholds were selected based on prior sleep literature, using amplitude gates of $-40 \pm 35\,\mu$V, a minimum peak-to-trough swing of $75\,\mu$V, and valid duration limits between 160–1700 ms [7].

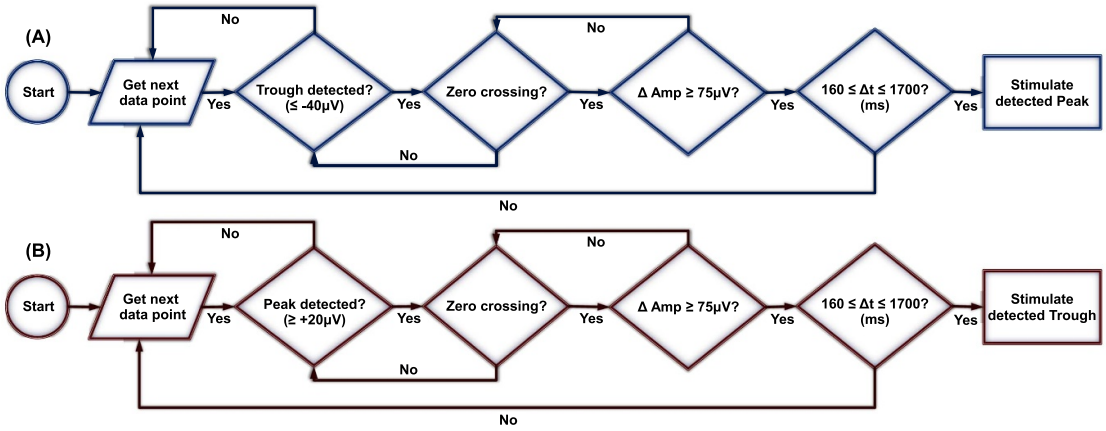

Figure 5. Online detection logic for delta wave extrema. Flowchart of the real-time event-based detection algorithm used for auditory stimulation delivery. Peaks and troughs of the delta wave are identified using predefined amplitude and duration thresholds applied to the filtered EEG signal. Detected extrema directly trigger auditory stimulation in a closed-loop manner, resulting in phase-targeted stimulation within predefined delta-cycle phase windows.

In the present work, the term *phase-targeted* refers to stimulation that is delivered at reproducible and predefined phase segments of the delta cycle (peak or trough), achieved through real-time, event-based detection of delta wave extrema rather than continuous phase estimation.

In ***in-phase*** **stimulation**, a trough was first identified when the signal dropped below $-40\,\mu$V. The algorithm then tracked the minimum amplitude and monitored the subsequent rise until the signal increased by at least $+75\,\mu$V above the trough and exceeded $+20\,\mu$V. If the trough-to-peak duration fell within 160–1700 ms, a peak was confirmed and an auditory stimulus was triggered.

In ***anti-phase*** **stimulation**, detection proceeded in the opposite direction. Once a positive half-wave exceeding $+20\,\mu$V was detected, the algorithm tracked the maximum amplitude until polarity reversed. When the waveform subsequently dropped $\geqslant 75\,\mu$V below the last peak and reached below $-40\,\mu$V within 160–1700 ms, a valid trough was identified and stimulation was delivered.

Zero-crossing guards of $\pm 5\,\mu$V were implemented between positive and negative phases to prevent false detections caused by small fluctuations around zero. The complete event-based detection logic for both in-phase and anti-phase conditions is summarized in figure 5.

At the start of each stimulation block, all detection flags (e.g. peak, trough, zero-crossing) were reset to their default states. This reset ensured that detection logic operates independently across blocks, preventing residual states or incomplete waveform transitions from previous blocks from triggering false detections.

Each confirmed detection sent a non-blocking signal to the audio thread for stimulus playback and logged an event code for synchronization with the EEG recording. To ensure precise synchronization between stimulation events and EEG recordings, each auditory stimulus was marked through both software and hardware triggers. When a valid detection occurred, the CLAS application logged an internal event code in parallel with the auditory playback and simultaneously activated an external trigger interface connected to the EGI amplifier (Digital Input (DIN) markers in figure 2). This interface generated a DIN pulse that was recorded in the NetStation Acquisition data stream, allowing the temporal alignment between detected delta wave phase and sound onset to be verified offline. System latency was evaluated by comparing the timestamps of internal and external markers, as reported in the Results section.

3.5. Auditory stimuli

Auditory stimuli consisted of short bursts of pink noise ($1/f$ noise), commonly used in CLAS paradigms [27, 29, 32, 37]. The pink noise bursts had a duration of 50 ms, with a 5 ms rising and falling ramp, respectively. Auditory playback was handled in real-time using the PyAudio library(version 0.2.13), which streamed preloaded pink-noise samples stored as 16-bit mono waveforms at a 16 kHz sampling rate. This configuration ensured low-latency output and precise temporal alignment between the software command and the generated sound. The headphones were connected to a trigger interface (AV Device DIN Adapter, Magstim EGI, Eugene, OR, USA), which acted as a relay between the stimulation software and the auditory output to ensure precise timing synchronization with EEG recordings. The temporal precision of the auditory triggers was verified using the AV Device Tester provided by Magstim EGI, which measures the accuracy of stimulus markers transmitted through the Net Amps DIN port and recorded with the EEG.

3.6. Participants

Nineteen healthy adults (5 males, 14 females; 5 men, 13 women, 1 non-binary; mean age = 23.79 ± 3.82 years) were recruited on a voluntary basis. Before participation, eligibility was verified by a member of the research team to ensure compliance with study criteria. Inclusion criteria were: age between 18 and 40 years, and adequate comprehension of either French or English. Exclusion criteria comprised a history of auditory disorders or hearing loss, diagnosed sleep disorders, chronic use of psychotropic medication, shift or night work within the past month, neurological or psychiatric conditions, and epilepsy. Participants were also instructed to abstain from alcohol on the day prior to and the day of data collection, to refrain from caffeine intake on the day of testing, and to avoid intense physical exercise on the afternoon preceding the recording session.

3.7. Data collection

This study has been reviewed and approved by the Research Ethics Board of the Centre Intégré Universitaire de Santé et des Services Sociaux du Nord-de-l'Île-de-Montréal (CIUSSS-NIM; MP-12-2022-2984), and data were collected at the Center for Advanced Research in Sleep Medicine (CARSM). Participants arrived at the sleep laboratory about 30 to 45 min before their usual bedtime and signed and informed consent was obtained before any further steps were taken. Head circumference was measured to select the appropriate EEG net size. The Cz electrode was located at the midpoint between the nasion-inion and ear-to-ear lines, marked on the scalp, and used to align a 128-channel gel-based EEG net. Recordings took place in a fully darkened, sound-attenuated bedroom. Impedances were maintained below 50 kΩ, signals were referenced online to Cz, and data were sampled at 1000 Hz.

Sound intensity was individually calibrated: participants listened to short pink-noise bursts and adjusted the volume to a level that was clearly perceptible but unlikely to cause arousal once asleep. This self-selected intensity was used for all stimulation blocks. Across participants, the final sound level typically corresponded to one to two volume bars on the experiment computer, representing low-intensity auditory stimulation.

Participants were then allowed to follow their usual bedtime routine. CLAS stimulation began once stage N3 sleep was visually identified in real-time by a trained experimenter, indicated by prominent delta waves (figure 2). Upon N3 detection, the CLAS application was activated and configured for a total of 15 min of stimulation divided into three 5 min conditions: *In-phase*, *Anti-phase*, and *Sham*. Auditory stimuli were presented binaurally through ER2XR insert earphones (Etymotic Research, IL, USA). Stimulation was paused whenever participants showed signs of arousal or transitioned out of N3, and resumed from the beginning upon re-entry into stable N3. Depending on the amount of stable delta wave activity, total stimulation time per participant ranged from a few minutes up to 45 min across multiple N3 cycles.

3.8. Final dataset and analysis overview

Of the 19 participants initially recruited, data from five participants were excluded from subsequent analyses because of either the use of an earlier version of the detection algorithm ($n = 2$) or the absence of stable N3 sleep with detectable delta waves ($n = 3$). Therefore, the final dataset included 14 participants (11 females and 3 males) who completed all three stimulation conditions (*In-phase*, *Anti-phase*, and *Sham*). All analyses reported below were conducted on this validated subset to evaluate the performance, latency, and stimulation accuracy of the CLAS-hdEEG system. Standard classification metrics were used to evaluate system performance, including precision, recall, and $F1$-score, computed from true-positive, false-positive, and false-negative counts as commonly defined. Specific definitions were adapted to each test (e.g. online/offline detection agreement vs phase-targeting success rate) and are described in their respective Results subsections.

4. Results

4.1. System performance

4.1.1. Latency between detection and stimulation

Previous CLAS studies have reported a variety of timing-related metrics, including phase alignment accuracy, stimulation efficiency, and algorithmic or computational delay, reflecting heterogeneity in how temporal performance is defined and evaluated across systems. Because timing performance is assessed using different operational definitions across the CLAS literature, we distinguish three conceptual levels of latency reporting, algorithmic, functional, and system-level, based on whether timing is evaluated through phase estimation accuracy, post-hoc physiological alignment, or system-level timing characterized using component-wise delay estimation or hardware-recorded event markers, ranging from stimulus-onset verification to explicit end-to-end quantification of detection-to-stimulation delay.

At the algorithmic level, temporal performance is implicitly assessed through the accuracy and computational efficiency of real-time phase estimation. Methods such as phase-locked loop tracking, predictive phase models, or instantaneous phase estimation algorithms quantify how precisely the phase of ongoing oscillations can be estimated under controlled signal-processing conditions. A representative example is provided by Ferster *et al* [53], who benchmarked phase estimation accuracy, robustness, and computational efficiency relative to offline ground-truth phase estimates. In this study,

algorithm execution efficiency on embedded hardware was evaluated by quantifying the number of processor cycles required per EEG sample, reflecting computational processing cost rather than physical detection-to-stimulation latency. These metrics characterize algorithmic and computational delay, but they do not incorporate delays introduced by EEG acquisition hardware, data buffering, operating system scheduling, or auditory stimulus delivery, and therefore do not provide a measure of physical detection-to-stimulation latency.

At the functional level, temporal accuracy is inferred indirectly by examining whether stimulation effects or evoked responses occur near the intended oscillatory phase. This includes post-hoc phase alignment analyses, zero-crossing–based timing evaluations, and event-related potential timing relative to stimulation. Several CLAS studies adopt this approach by applying protocol-defined delays or phase-targeting rules and subsequently assessing whether auditory stimulation coincides with the desired wave features [32, 50, 51, 55, 56]. While these analyses provide valuable information about physiological relevance and phase-targeting efficacy, they rely on inferred timing relationships and do not constitute a direct measurement of the physical delay between neural event detection and auditory output.

At the system level, latency refers to the delay between the online detection of a neural event and the onset of the corresponding auditory stimulus, encompassing contributions from signal acquisition, real-time processing, operating system scheduling, audio drivers, and digital-to-analog conversion. This definition reflects the cumulative impact of hardware and software components involved in real-time stimulation delivery.

Several recent studies have documented system timing by integrating stimulation triggers or auditory onset markers into the EEG recording. For example, Krugliakova *et al* [39] and Leach *et al* [41] recorded stimulation triggers as digital inputs to the EGI amplifier, enabling alignment of EEG activity with stimulation timing and subsequent offline evaluation of phase-targeting accuracy. Similarly, Hebron *et al* [42] used a hardware TriggerBox to insert auditory onset markers into the EEG data stream, allowing precise temporal alignment between EEG signals and sound onset for phase-based analyses. These approaches provide system-level timing information and support validation of phase-targeted stimulation, although they do not report a numerical detection-to-sound delay in milliseconds. A different approach was adopted by Valenchon *et al* [54], who reported system latency in a wearable closed-loop platform by estimating the contribution of individual processing components, including filtering, inference, and stimulation hardware delays, resulting in a total estimated detection-to-stimulation delay of approximately 64 ms, derived from component-wise delay estimates rather than direct measurement of auditory onset. This approach characterizes system latency through component-wise estimation rather than through direct measurement of auditory onset timing recorded within the EEG.

In the present study, system-level latency was quantified by comparing internal detection timestamps generated by the CLAS-hdEEG system with externally generated markers corresponding to the physical onset of auditory stimulation recorded by the EEG amplifier. Auditory onset markers were generated using a Magstim EGI AV device tester, a hardware tool specifically designed for scientific verification of stimulus timing in real-time EEG experiments, enabling precise and reproducible measurement of detection-to-stimulation latency. This procedure enabled direct quantification of the detection-to-stimulation delay under the implemented experimental configuration. Across all stimulation blocks, the mean latency was 20.03 ± 0.5 ms (range: 19.03–21.01 ms). While absolute latency values depend on system architecture and implementation choices, this delay corresponds to less than 20% of a delta wave cycle at 4 Hz and remains compatible with phase-targeted delta wave stimulation.

4.1.2. Online versus offline filtering performance

To validate the real-time moving-average implementation, online-filtered Fz signals (sampled at 500 Hz) were compared with offline zero-phase fourth-order Butterworth band-pass filters (0.25–9 Hz) applied after recording to the same downsampled data. After discarding the first 2 s to exclude filter initialization transients, correlation coefficients were computed between the online and offline traces across all stimulation blocks and averaged per subject.

Across participants ($n = 14$), the online-filtered signals showed high correspondence with the offline reference ($r = 0.83 \pm 0.07$), confirming that the real-time implementation accurately reproduced the offline filtering behavior while maintaining stable temporal characteristics. Participant-wise correlation values are presented in table 1. These results validate the fidelity of the implemented moving-average filters for real-time EEG processing and ensure that subsequent delta wave detection was based on physiologically equivalent signals.

4.2. Detection accuracy

4.2.1. Phase-targeting success rate

To evaluate the temporal accuracy of auditory stimulation delivery, we computed the proportion of stimuli delivered within the predefined target phase windows among all delivered events (phase-targeting success rate). A stimulation was classified as *successful* when the auditory burst occurred within the predefined 90° phase window of the delta wave (0°–90° for in-phase blocks; 180°–270° for anti-phase blocks), after correcting for the measured system

Table 1. Per-subject correlation (r) between online and offline filtered Fz signals.

Subject	Mean r	SD r	Subject	Mean r	SD r
03	0.60	0.26	12	0.81	0.16
04	0.87	0.03	13	0.85	0.03
07	0.89	0.03	14	0.79	0.08
08	0.84	0.06	15	0.85	0.16
09	0.87	0.05	16	0.67	0.03
10	0.84	0.04	17	0.78	0.06
11	0.87	0.05	18	0.87	0.05
		Average:	0.83 ± 0.07		

*Note.*Correlation coefficients (r) represent the agreement between online (real-time) and offline (zero-phase) filtered Fz signals for each participant. Mean and standard deviation (SD) were computed across all stimulation blocks.

Table 2. Phase-targeting success rate per participant.

Subject	TP	Total	Success rate	Subject	TP	Total	Success rate
03	843	942	0.895	12	451	478	0.944
04	342	373	0.917	13	788	905	0.871
07	945	1019	0.927	14	458	493	0.929
08	378	437	0.865	15	823	858	0.959
09	528	575	0.918	16	411	443	0.928
10	204	247	0.826	17	651	708	0.919
11	956	1029	0.929	18	452	509	0.888
			Mean $\pm$ SD $= 0.908 \pm 0.036$				
			Total $= 9016$	TP $= 8230$	Pooled success rate $= 0.913$		

*Note.*TP = true positives. Total = number of auditory stimulations delivered. Success rate represents the proportion of correctly phase-targeted stimulations among all delivered auditory events. Mean $\pm$ SD reflects between-subject variability across participants ($n = 14$). Pooled success rate represents the proportion computed across all stimulation events.

delay of 20 ms. Stimulations meeting these criteria were considered *true positives* (TP), whereas stimulations falling outside the targeted phase range were labeled as *false positives* (FP). The total number of delivered stimuli (TP + FP) was used to compute the proportion of correctly phase-targeted stimulations, referred to as the phase-targeting success rate.

Across participants, the mean success rate was 0.908 ± 0.036 (mean $\pm$ SD), with participant-level success rates ranging from 0.826 to 0.959. The pooled success rate across all stimulation events was 0.913, computed as the ratio of the total number of successfully phase-targeted stimulations to the total number of delivered stimulations across all participants.

This indicates that approximately 91% of all auditory stimulations were delivered within the intended 90° phase window of the ongoing delta wave. Participant-wise success rates are shown in table 2. These results confirm stable phase-targeted performance across recording sessions and subjects.

4.2.2. Comparison with offline detection

To evaluate the reliability of the real-time detection algorithm, offline delta wave detection was performed on the same raw EEG segments using the same amplitude and duration criteria employed online. Each stimulation block was first band-pass filtered offline (0.5–4 Hz, fourth-order Butterworth, zero-phase) and then segmented into individual delta waves based on peak-to-peak amplitude 75 μV thresholds, negative and positive deflection $-40 \pm 35\,\mu$V, and duration of 160–1700 ms, consistent with standard delta wave detection criteria in the literature [57].

For each offline-detected delta wave, the corresponding stimulation markers from the CLAS system were inspected to determine whether the real-time algorithm identified and stimulated the same event. Because stimulation triggers occurred with a fixed hardware delay of 20 ms, the expected onset of the auditory pulse was adjusted accordingly. A stimulation was considered a true positive (TP) if its trigger occurred within the temporal boundaries of the offline-detected delta wave and matched the targeted phase (peak or trough, depending on the stimulation condition). Offline waves without a corresponding stimulation were labeled as false negatives (FN), and stimulations without a matching offline delta wave were labeled as false positives (FP). From these counts, we computed the precision, recall, and $F1$-score for each block and stimulation condition.

Across all sessions and participants, the real-time detection algorithm achieved a mean precision of

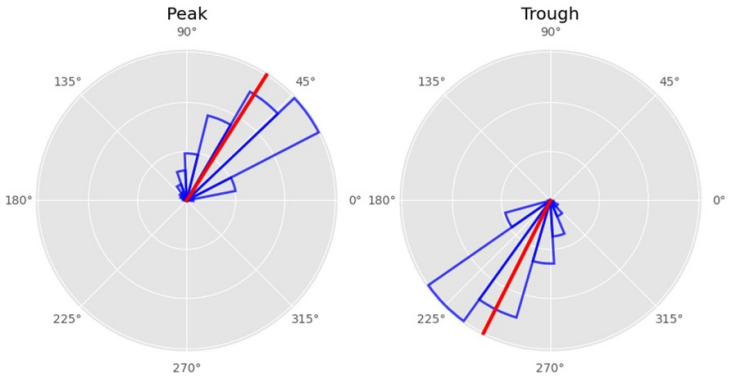

Figure 6. Phase alignment of auditory stimulation. Circular histograms showing the distribution of instantaneous delta wave phases at stimulation onset for *in-phase* stimulation (left) and *anti-phase* stimulation (right). Each blue trace represents the normalized occurrence of stimulations per angular bin (20° steps). Red lines indicate the mean resultant phase across all events. Stimulations occurred within the expected phase windows—near the positive half-wave ($0° - 90°$) for in-phase condition and the negative half-wave ($180° - 270°$) for anti-phase condition, demonstrating consistent phase-targeted stimulation at the target delta wave segments following event-based detection.

≈0.76, recall of ≈0.85, and $F1$-score of ≈0.80, indicating a strong agreement between online and offline detections. This confirms that the implemented real-time algorithm closely reproduces the performance of offline gold-standard detection, despite operating under real-time constraints.

4.2.3. Phase alignment of auditory stimulation

To quantify the phase specificity of the stimulation delivery, the instantaneous phase of each detected delta wave was extracted *offline* from the filtered Fz signal at the moment of auditory onset. Phases were computed using the Hilbert transform and expressed in degrees, where 0° corresponds to the positive-to-negative zero crossing, 90° to the positive peak, 180° to the negative-to-positive zero crossing, and 270° to the trough of the delta wave. Circular histograms were constructed across all stimulation events for both *in-phase* stimulation and *anti-phase* stimulation, with a bin width of 20° (figure 6).

In the ***in-phase* condition**, stimulation phases were concentrated within 0° to 90°, with a mean resultant phase of ∼51° (circular variance ∼0.10), indicating that auditory stimuli occurred during the ascending portion of the positive half-wave and near the peak extremum.

In the ***anti-phase* condition**, stimulation phases were concentrated within 180° to 270°, with a mean resultant phase of ∼243° (circular variance ∼0.087), consistent with stimulation occurring on the descending portion of the negative half-wave and near the trough extremum.

These results indicate that the CLAS algorithm accurately targets the intended phase segment of ongoing delta waves, while maintaining consistent phase-targeted stimulation across conditions, as verified by offline phase analysis.

Although phase clustering was consistent across participants ($n = 14$), future studies including larger samples may further refine variance estimates and strengthen statistical confidence in phase-alignment metrics.

5. Discussion

To the best of our knowledge, this study introduces and validates the first CLAS-hdEEG system designed for real-time delta wave detection and phase-targeted sound delivery fully integrated within the Magstim EGI environment, with explicit end-to-end latency validation. This framework integrates 128-channel EEG acquisition with low-latency auditory stimulation, achieving millisecond-scale detection-to-stimulation latency from neural detection to sound onset. This demonstrates that hd-EEG recording and real-time stimulation can be combined without compromising temporal accuracy, which is an important step forward given the computational and synchronization challenges traditionally associated with high-channel count systems.

While previous studies have used open-loop rhythmic stimulation paradigms such as the ASSR [38] to characterize how the brain entrains to periodic sounds, the present system enables a causal, phase-specific modulation of endogenous delta waves in real-time. This closed-loop framework thus transitions from measuring auditory entrainment to actively shaping ongoing delta wave dynamics, opening the door to mechanistic investigations of sensory–neural interactions during sleep and sedation.

By coupling precise temporal control with high spatial resolution, this framework enables detailed exploration of how delta wave activity propagates and adapts in response to auditory stimulation across cortical regions. Future developments may

include integrating adaptive, machine learning–based detection strategies to enhance sensitivity and context awareness beyond classical threshold-based criteria. Altogether, these results establish a technically robust and temporally precise foundation for future studies investigating large-scale brain dynamics and their modulation through phase-targeted stimulation.

Beyond its technical validation, this platform offers the possibility of examining how phase-targeted auditory stimulation interacts with delta waves in different situations, such as pharmacologically induced sedation or unconsciousness. CLAS has recently been shown to alter slow-wave homeostasis during dexmedetomidine sedation, suggesting that auditory neuromodulation can operate even when delta waves are pharmacologically driven [58, 59]. In parallel, our team has recently proposed a protocol for the integration of CLAS during propofol general anesthesia to directly test its impact on the anesthetic delta waves and nociception-related dynamics [60]. The temporal precision and spatial coverage afforded by the present CLAS-hdEEG system provide the necessary framework to rigorously evaluate such translational applications under controlled conditions. If phase-targeted stimulation can reliably reinforce pharmacologically induced delta waves, it could ultimately complement balanced anesthesia strategies by strengthening endogenous oscillatory dynamics without increasing pharmacological drug dosage.

In addition, the integration of hd-EEG allows us to consider spatial organization of delta waves. Slow oscillations are not static events, as they emerge and propagate across cortical networks, and their spatial characteristics differ between natural sleep and anesthetic-induced unconsciousness [2, 61]. By capturing whole-brain activity with high spatial resolution while maintaining millisecond-scale detection-to-stimulation latency, this system enables the identification of consistent initiation sites or propagation pathways that may represent optimal targets for stimulation. Determining whether specific cortical regions serve as more effective entry points for closed-loop modulation could refine stimulation strategies in all clinical contexts in which slow-wave dynamics play a central role.

6. Conclusion

This study introduces and validates a novel CLAS-hdEEG system capable of real-time, phase-targeted auditory stimulation using hd-EEG. When evaluated during N3 sleep in 14 healthy subjects, the CLAS-hdEEG system achieved a mean detection-to-stimulation latency of approximately 20 ms, stable event-based targeting of delta wave extrema within predefined 90° phase windows, and strong agreement between online and offline detections, with a mean precision of ≈0.76, recall of ≈0.85, and an $F1$-score of ≈0.80, all criteria essential for closed-loop paradigms. By providing a validated framework for integrating acquisition, detection, and stimulation, this work paves the way for future research examining the neural mechanisms and clinical applications of delta wave modulation in altered states of consciousness.

Acknowledgments

We would like to thank the members of the Neurophysiology of Altered Consciousness and Critical Care (NAC^3) laboratory for their help and contribution to the data collection. We also acknowledge and thank the funding sources listed below.

Data availability statement

The data cannot be made publicly available upon publication because they contain sensitive personal information. The data that support the findings of this study are available upon reasonable request from the authors.

Funding

This work was supported by the Future Leaders in Canadian Brain Research Grant from the Brain Canada Foundation, by a Pilot Project Grant from the Québec Sleep Research Network (a thematic network funded by the Fonds de recherche du Québec—Santé (FRQS)), a Discovery Grant and Launch Supplement from the Natural Sciences and Engineering Research Council of Canada (NSERC) (RGPIN-2022–04220), by a Junior 1 Research Scholars Award and Establishment of Young Researchers Supplement from the FRQS, by the John R Evans Leaders Fund from the Canadian Foundation for Innovation (CFI), by the CIFAR-Azrieli Global Scholars Program from CIFAR, and by the Research Center of the Centre intégré universitaire de santé et de services sociaux du Nord-de-l'Île-de-Montréal. Additional funds came from the Faculty of Medicine of Université de Montréal (Bourse de la Relève; studentship to CPR), and the Department of Neuroscience of Université de Montréal (Bourse de recrutement; studentship to CPR).

Conflict of interest

The authors declare that there are no conflicts of interest related to this work.

Use of generative AI

Generative artificial intelligence tools were used to improve the clarity and grammar of the text. No AI systems were used for coding, data analysis,

figure generation, or interpretation of results, and all scientific content was written and verified by the authors.

Ethical statement

This study was performed in accordance with the Declaration of Helsinki. This human study was approved by the Research Ethics Board of the Centre Intégré Universitaire de Santé et des Services Sociaux du Nord-de-l'Île-de-Montréal—approval: MP-32-2023-2523. All adult participants provided written informed consent to participate in this study.

Author contributions

Hanieh Bazregarzadeh 0009-0003-4254-7530
Conceptualization (equal), Data curation (equal), Formal analysis (equal), Investigation (equal), Methodology (equal), Software (equal), Validation (equal), Visualization (equal), Writing – original draft (equal), Writing – review & editing (equal)

Clara Pic Roca 0009-0001-8329-9292
Conceptualization (equal), Data curation (equal), Visualization (equal), Writing – original draft (equal), Writing – review & editing (equal)

Antonio Martin 0000-0002-7528-9246
Writing – review & editing (equal)

Karine Lacourse 0000-0001-8488-7312
Writing – review & editing (equal)

Jean-Marc Lina
Funding acquisition (equal), Supervision (equal)

Julie Carrier 0000-0001-5311-2370
Funding acquisition (equal), Supervision (equal)

Catherine Duclos 0000-0002-8406-5228
Conceptualization (equal), Funding acquisition (equal), Methodology (equal), Project administration (equal), Supervision (equal), Writing – review & editing (equal)

References

[1] Steriade M, McCormick D A and Sejnowski T J 1993 Thalamocortical oscillations in the sleeping and aroused brain *Science* **262** 679–85
[2] Massimini M, Huber R, Ferrarelli F, Hill S and Tononi G 2004 The sleep slow oscillation as a traveling wave *J. Neurosci.* **24** 6862–70
[3] Uygun D S and Basheer R 2022 Circuits and components of delta wave regulation *Brain Res. Bull.* **188** 223–32
[4] Steriade M, Nunez A and Amzica F 1993 A novel slow (< 1 Hz) oscillation of neocortical neurons *in vivo*: depolarizing and hyperpolarizing components *J. Neurosci.* **13** 3252–65
[5] Timofeev I, Grenier F and Steriade M 2001 Disfacilitation and active inhibition in the neocortex during the natural sleep-wake cycle: an intracellular study *Proc. Natl Acad. Sci.* **98** 1924–9
[6] Reto Huber M F G, Massimini M and Tononi G 2004 Local sleep and learning *Nature* **430** 78–81
[7] Riedner B A, Vyazovskiy V V, Huber R, Massimini M, Esser S, Murphy M and Tononi G 2007 Sleep homeostasis and cortical synchronization: III. A high-density EEG study of sleep slow waves in humans *Sleep* **30** 1643–57
[8] Santostasi G, Malkani R, Riedner B, Bellesi M, Tononi G, Paller K A and Zee P C 2016 Phase-locked loop for precisely timed acoustic stimulation during sleep *J. Neurosci. Methods* **259** 101–14
[9] Ngo H-V V, Antony J W and Rasch B 2022 Real-time stimulation during sleep: prior findings, novel developments and future perspectives *J. Sleep Res.* **31** e13735
[10] Esfahani M J, Farboud S, Ngo H-V V, Schneider J, Weber F D, Talamini L M and Dresler M 2023 Closed-loop auditory stimulation of sleep slow oscillations: basic principles and best practices *Neurosci. Biobehav. Rev.* **153** 105379
[11] Tononi G and Cirelli C 2006 Sleep function and synaptic homeostasis *Sleep Med. Rev.* **10** 49–62
[12] Diekelmann S and Born J 2010 The memory function of sleep *Nat. Rev. Neurosci.* **11** 114–26
[13] Tononi G and Cirelli C 2014 Sleep and the price of plasticity: from synaptic and cellular homeostasis to memory consolidation and integration *Neuron* **81** 12–34
[14] Mölle M, Marshall L, Gais S and Born J 2002 Grouping of spindle activity during slow oscillations in human non-rapid eye movement sleep *J. Neurosci.* **22** 10941–7
[15] Staresina B P, Bergmann T O, Bonnefond M, Meij R V D, Jensen O, Deuker L, Elger C E, Axmacher N and Fell J 2015 Hierarchical nesting of slow oscillations, spindles and ripples in the human hippocampus during sleep *Nat. Neurosci.* **18** 1679–86
[16] Helfrich R F, Mander B A, Jagust W J, Knight R T and Walker M P 2018 Old brains come uncoupled in sleep: slow wave-spindle synchrony, brain atrophy and forgetting *Neuron* **97** 221–30
[17] Dijk D-J 2009 Regulation and functional correlates of slow wave sleep *J. Clin. Sleep Med.* **5** S6–S15
[18] Xie L *et al* 2013 Sleep drives metabolite clearance from the adult brain *Science* **342** 373–7
[19] Besedovsky L, Lange T and Born J 2012 Sleep and immune function *Pflügers Archiv-European J. Physiol.* **463** 121–37
[20] Hao C, Mingzhu Li, Ning Q and Ning M 2023 One night of 10-h sleep restores vigilance after total sleep deprivation: the role of delta and theta power during recovery sleep *Sleep Biol. Rhythm.* **21** 165–73
[21] Carrier J, Land S, Buysse D J, Kupfer D J and Monk T H 2001 The effects of age and gender on sleep EEG power spectral density in the middle years of life (ages 20–60 years old) *Psychophysiology* **38** 232–42
[22] Feige B, Baglioni C, Spiegelhalder K, Hirscher V, Nissen C and Riemann D 2013 The microstructure of sleep in primary insomnia: an overview and extension *Int. J. Psychophysiol.* **89** 171–80
[23] Mander B A, Marks S M, Vogel J W, Rao V, Brandon L, Saletin J M, Ancoli-Israel S, Jagust W J and Walker M P 2015 β-amyloid disrupts human NREM slow waves and related hippocampus-dependent memory consolidation *Nat. Neurosci.* **18** 1051–7
[24] Marshall L, Helgadóttir H, Mölle M and Born J 2006 Boosting slow oscillations during sleep potentiates memory *Nature* **444** 610–3
[25] Massimini M, Ferrarelli F, Esser S K, Riedner B A, Huber R, Murphy M, Peterson M J and Tononi G 2007 Triggering sleep slow waves by transcranial magnetic stimulation *Proc. Natl Acad. Sci.* **104** 8496–501
[26] Zhao X *et al* 2024 Restoration of abnormal sleep EEG power in patients with insomnia disorder after 1Hz rTMS over left DLPFC *Front. Psychiatry* **15** 1431837
[27] Ngo H-V V, Martinetz T, Born J and Mölle M 2013 Auditory closed-loop stimulation of the sleep slow oscillation enhances memory *Neuron* **78** 545–53

[28] Ong J L, June C L, Chee N I Y N, Santostasi G, Paller K A, Zee P C and Chee M W L 2016 Effects of phase-locked acoustic stimulation during a nap on EEG spectra and declarative memory consolidation *Sleep Med.* **20** 88–97
[29] Besedovsky L, Ngo H-V V, Dimitrov S, Gassenmaier C, Lehmann R and Born J 2017 Auditory closed-loop stimulation of EEG slow oscillations strengthens sleep and signs of its immune-supportive function *Nat. Commun.* **8** 1984
[30] Papalambros N A, Santostasi G, Malkani R G, Braun R, Weintraub S, Paller K A and Zee P C 2017 Acoustic enhancement of sleep slow oscillations and concomitant memory improvement in older adults *Front. Hum. Neurosci.* **11** 247563
[31] Papalambros N A, Weintraub S, Chen T, Grimaldi D, Santostasi G, Paller K A, Zee P C and Malkani R G 2019 Acoustic enhancement of sleep slow oscillations in mild cognitive impairment *Ann. Clin. Transl. Neurol.* **6** 1191–201
[32] Navarrete M, Schneider J, Ngo H-V V, Valderrama M, Casson A J and Lewis P A 2020 Examining the optimal timing for closed-loop auditory stimulation of slow-wave sleep in young and older adults *Sleep* **43** zsz315
[33] Zeller C J, Wunderlin M, Wicki K, Teunissen C E, Nissen C, Züst M A and Klöppel S 2024 Multi-night acoustic stimulation is associated with better sleep, amyloid dynamics and memory in older adults with cognitive impairment *GeroScience* **46** 6157–72
[34] Jourde H R, Merlo R, Brooks M, Rowe M and Coffey E B J 2023 The neurophysiology of closed-loop auditory stimulation in sleep: a magnetoencephalography study *Eur. J. Neurosci.* **59** ejn.16132
[35] Fehér K D, Wunderlin M, Maier J G, Hertenstein E, Schneider C L, Mikutta C, Züst M A, Klöppel S and Nissen C 2021 Shaping the slow waves of sleep: a systematic and integrative review of sleep slow wave modulation in humans using non-invasive brain stimulation *Sleep Med. Rev.* **58** 101438
[36] Harlow T J, Jané M B, Read H L and Chrobak J J 2023 Memory retention following acoustic stimulation in slow-wave sleep: a meta-analytic review of replicability and measurement quality *Front. Sleep* **2** 1082253
[37] Ngo H-V V, Miedema A, Faude I, Martinetz T, Mölle M and Born J 2015 Driving sleep slow oscillations by auditory closed-loop stimulation—a self-limiting process *J. Neurosci.* **35** 6630–8
[38] Lustenberger C, Patel Y A, Alagapan S, Page J M, Price B, Boyle M R and Fröhlich F 2018 High-density EEG characterization of brain responses to auditory rhythmic stimuli during wakefulness and NREM sleep *Neuroimage* **169** 57–68
[39] Krugliakova E, Skorucak J, Sousouri G, Leach S, Snipes S, Ferster M L, Poian G D, Karlen W and Huber R 2022 Boosting recovery during sleep by means of auditory stimulation *Front. Neurosci.* **16** 755958
[40] Huwiler S *et al* 2022 Effects of auditory sleep modulation approaches on brain oscillatory and cardiovascular dynamics *Sleep* **45** zsac155
[41] Leach S *et al* 2024 Acoustically evoked K-complexes together with sleep spindles boost verbal declarative memory consolidation in healthy adults *Sci. Rep.* **14** 19184
[42] Hebron H, Lugli B, Dimitrova R, Jaramillo V, Yeh L R, Rhodes E, Grossman N, Dijk D-J and Violante I R 2024 A closed-loop auditory stimulation approach selectively modulates alpha oscillations and sleep onset dynamics in humans *PLoS Biol.* **22** e3002651
[43] Murphy M, Riedner B A, Huber R, Massimini M, Ferrarelli F and Tononi G 2009 Source modeling sleep slow waves *Proc. Natl Acad. Sci.* **106** 1608–13
[44] Nir Y, Staba R J, Andrillon T, Vyazovskiy V V, Cirelli C, Fried I and Tononi G 2011 Regional slow waves and spindles in human sleep *Neuron* **70** 153–69
[45] Siclari F, Bernardi G, Riedner B A, LaRocque J J, Benca R M and Tononi G 2014 Two distinct synchronization processes in the transition to sleep: a high-density electroencephalographic study *Sleep* **37** 1621–37
[46] Mensen A, Riedner B and Tononi G 2016 Optimizing detection and analysis of slow waves in sleep EEG *J. Neurosci. Methods* **274** 1–12
[47] Massimini M, Ferrarelli F, Huber R, Esser S K, Singh H and Tononi G 2005 Breakdown of cortical effective connectivity during sleep *Science* **309** 2228–32
[48] Boveroux P *et al* 2010 Breakdown of within- and between-network resting state functional magnetic resonance imaging connectivity during propofol-induced loss of consciousness *Anesthesiology* **113** 1038–53
[49] Boly M *et al* 2012 Connectivity changes underlying spectral EEG changes during propofol-induced loss of consciousness *J. Neurosci.* **32** 7082–90
[50] Debellemaniere E, Chambon S, Pinaud C, Thorey V, Dehaene D, Léger D, Chennaoui M, Arnal P J and Galtier M N 2018 Performance of an ambulatory dry-EEG device for auditory closed-loop stimulation of sleep slow oscillations in the home environment *Front. Hum. Neurosci.* **12** 314779
[51] Garcia-Molina G *et al* 2018 Closed-loop system to enhance slow-wave activity *J. Neural Eng.* **15** 066018
[52] Henin S *et al* 2019 Closed-loop acoustic stimulation enhances sleep oscillations but not memory performance *Eneuro* **6** 2019
[53] Ferster M L, Poian G D, Menachery K, Schreiner S J, Lustenberger C, Maric A, Huber R, Baumann C R and Karlen W 2022 Benchmarking real-time algorithms for in-phase auditory stimulation of low amplitude slow waves with wearable EEG devices during sleep *IEEE Trans. Biomed. Eng.* **69** 2916–25
[54] Valenchon N, Bouteiller Y, Jourde H R, L'Heureux X, Sobral M, Coffey E B J and Beltrame G 2022 The portiloop: a deep learning-based open science tool for closed-loop brain stimulation *PLoS One* **17** e0270696
[55] Schneider J, Lewis P A, Koester D, Born J and Ngo H-V V 2020 Susceptibility to auditory closed-loop stimulation of sleep slow oscillations changes with age *Sleep* **43** zsaa111
[56] Bressler S, Neely R, Yost R M and Wang D 2024 A randomized controlled trial of alpha phase-locked auditory stimulation to treat symptoms of sleep onset insomnia *Sci. Rep.* **14** 13039
[57] Bouchard M, Lina J-M, Gaudreault P-O, Lafrenière A, Dubé J, Gosselin N and Carrier J 2021 Sleeping at the switch *Elife* **10** e64337
[58] Guay C S, Labonte A K, Montana M C, Landsness E C, Lucey B P, Kafashan M, Haroutounian S, Avidan M S, Brown E N and Palanca B J A 2021 Closed-Loop Acoustic Stimulation During Sedation with Dexmedetomidine (CLASS-D): protocol for a within-subject, crossover, controlled, interventional trial with healthy volunteers *Nat. Sci. Sleep* **13** 303–13
[59] Smith S K, Kafashan M M, Rios R L, Brown E N, Landsness E C, Guay C S and Palanca B J A 2024 Daytime dexmedetomidine sedation with closed-loop acoustic stimulation alters slow wave sleep homeostasis in healthy adults *BJA Open* **10** 100276
[60] Roca C P, Bazregarzadeh H, Morisson L, Martin A, Verdonck O, Gibbs S, LINA J-M, Carrier J, Richebé P and Duclos C 2026 Protocol for modulating anesthesia delta oscillations using closed loop auditory stimulation *Front. Hum. Neurosci.* **20** 1748528
[61] Murphy M *et al* 2011 Propofol anesthesia and sleep: a high-density EEG study *Sleep* **34** 283–91